

Figure S1. Structure of the *rsu-1* locus.

The *rsu-1(tm6690)* mutant harbors a 778-bp deletion at the 5'-end of the locus.

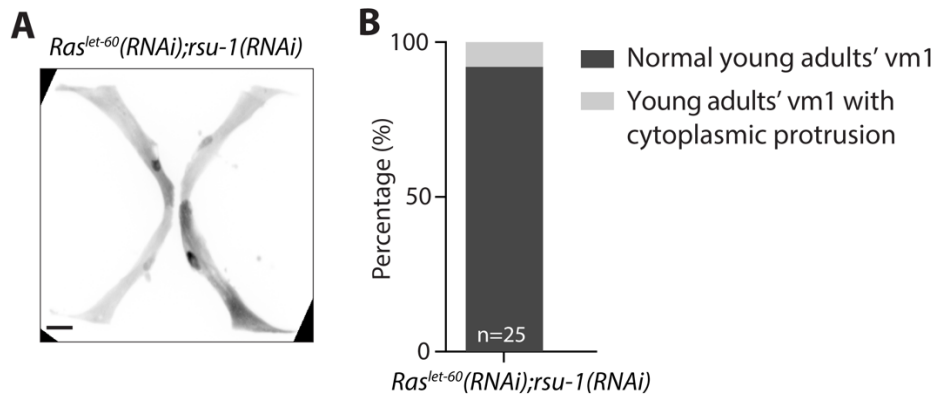


Figure S2. Depletion of Ras^{LET-60} and RSU-1 suppresses cytoplasmic protrusions in *rsu-1(tm6690)*.

- (A) Representative confocal images of *Pegl-15::GFP;Ras^{let-60}(RNAi);rsu-1(RNAi)*. Scale bar, 10 μ m.
- (B) Percentage of vulval muscle showing cytoplasmic protrusions in *rsu-1(RNAi);Ras^{let-60}(RNAi)*.

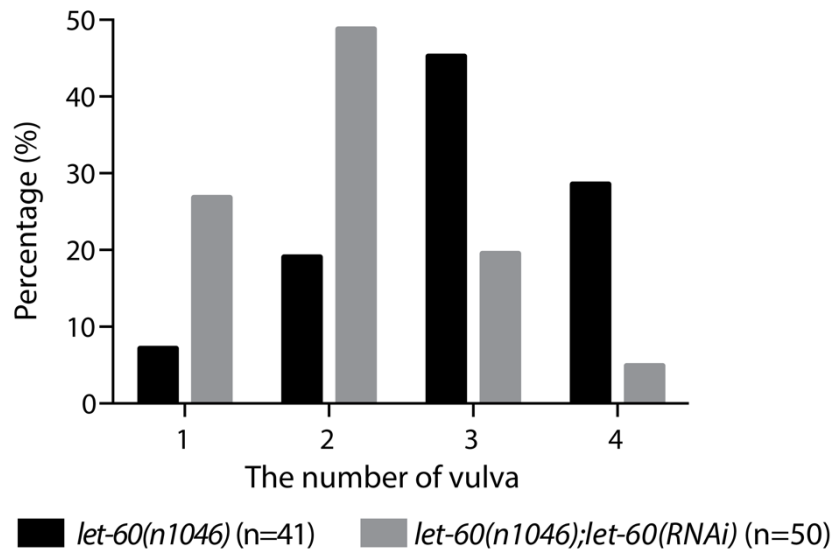


Figure S3. Depletion of Ras^{LET-60} suppresses the multivulva in *let-60(n1046)*.

Ratio of different vulva worm in *let-60(n1046)* and *let-60(n1046);Ras^{let-60}(RNAi)*.

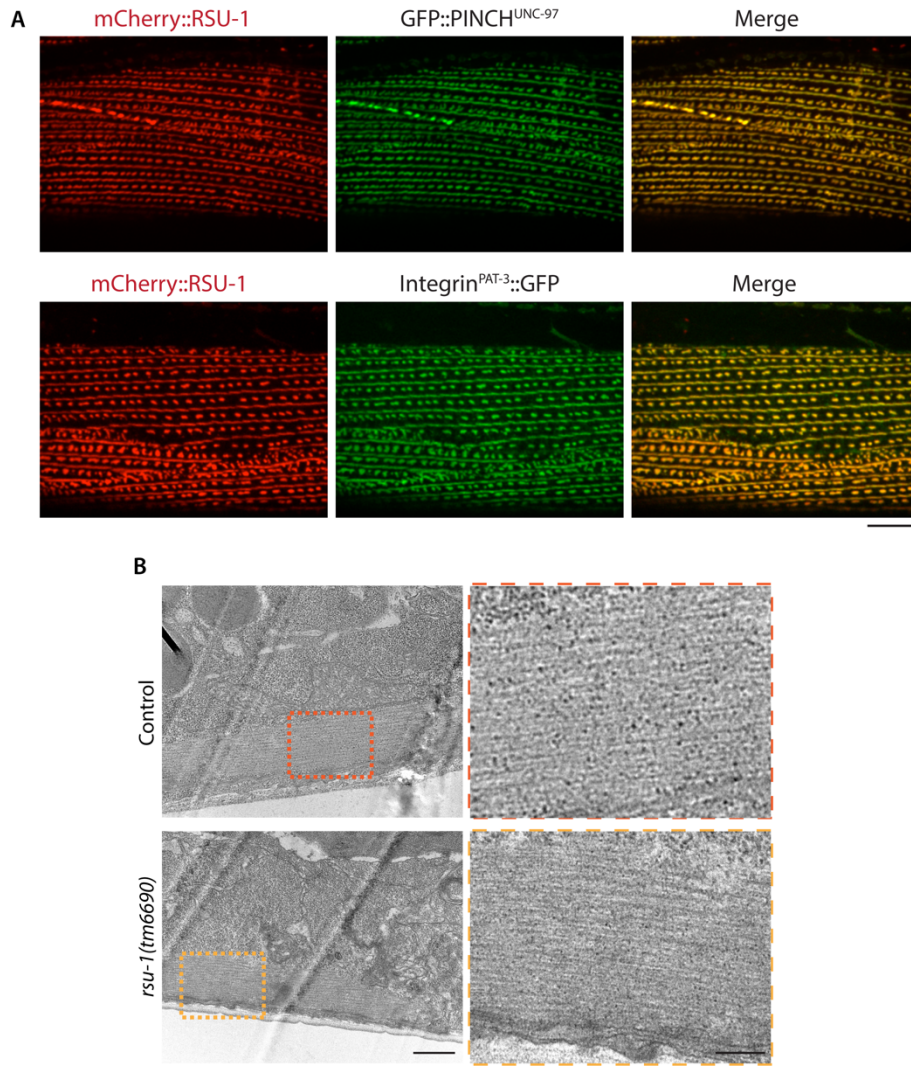


Figure S4. RSU-1 does not regulate subcellular localization of Integrin^{PAT-3} and PINCH^{UNC-97}.

(A) Representative confocal images of mCherry::RSU-1;GFP::PINCH^{UNC-97} and mCherry::RSU-1;Integrin^{PAT-3}::GFP in body-wall muscles. Scale bar, 10 μ m.

(B) Representative TEM images of body-wall muscle in control and *rsu-1(tm6690)*. Scale bar, 10 and 5 μ m.

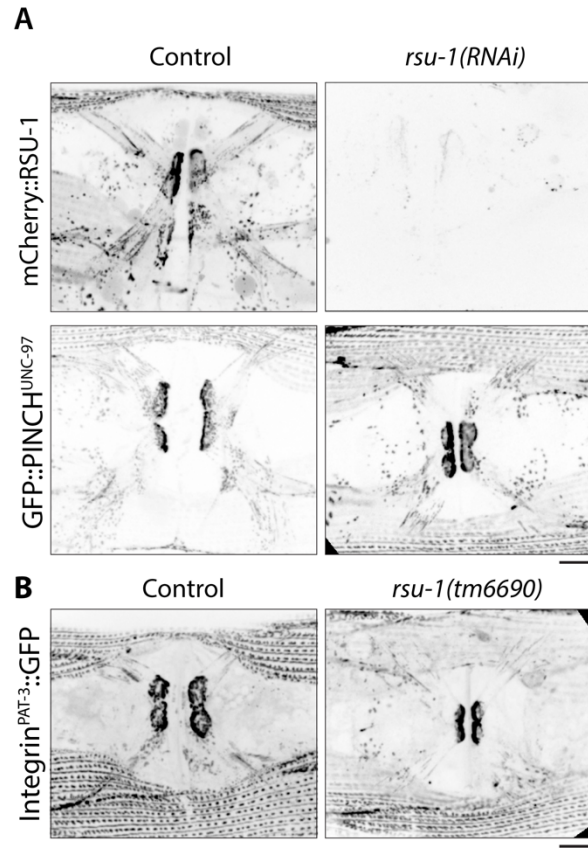


Figure S5. Depletion of RSU-1 does not change the focal adhesion sites in vulval muscle.

(A) Representative confocal images of mCherry::RSU-1 and mCherry::RSU-1;*rsu-1(RNAi)*.

Representative confocal images of GFP::PINCH^{UNC-97}, GFP::PINCH^{UNC-97};*rsu-1(RNAi)*.

Scale bar, 10 μ m.

(B) Representative confocal images of Integrin^{PAT-3}::GFP, and Integrin^{PAT-3}::GFP;*rsu-*

1(tm6690). Scale bar, 10 μ m.

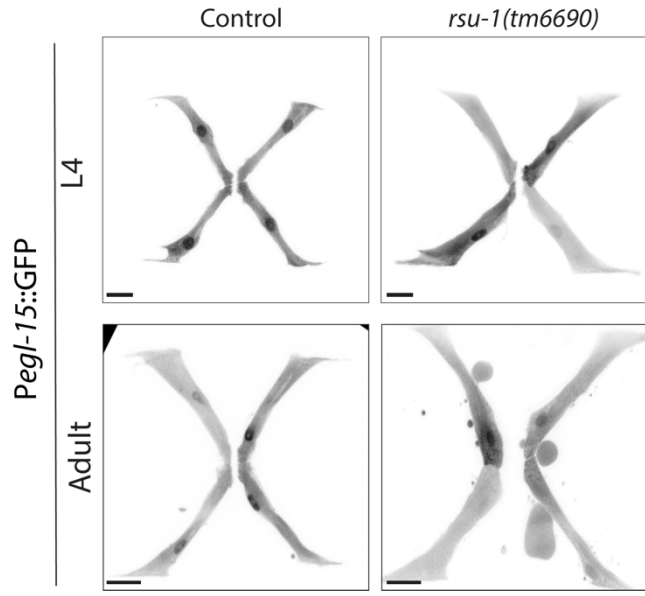


Figure S6. The morphology of vm1 muscle cells in L4 stage and adult stage.

Representative confocal images of *Pegl-15*::GFP and *Pegl-15*::GFP; *rsu-1*(*tm6690*) in L4 stage and adult stage. Scale bar, 10 μ m.